Modern Physics Letters B, Vol. 5, No. 22 (1991) 1533–1542

TRANSIENT AND STEADY STATE PROPERTIES OF THE INVERSE FARADAY EFFECT — SIMULATION AND THEORY

M. W. EVANS
433 Cornell Theory Center,
Ithaca, NY 14853, USA

Received 8 March 1991

A computer simulation of the inverse Faraday effect in a chiral and achiral ensemble has shown the presence of dynamic magnetisation and second order orientational rise/fall transients due to the conjugate product of a circularly polarised visible frequency laser pulse. Neither effect is known analytically, and the simulated transients are potentially directly comparable with experimental data using modified Kerr effect apparatus.

1. Introduction

The inverse Faraday effect (IFE) was first demonstrated theoretically[1] and experimentally[2,3] by Pershan and coworkers, and describes bulk magnetisation due to the conjugate product of a visible frequency circularly polarised pump laser pulse.[4,5] Atkins and Miller[6] later showed theoretically that the magnetisation is accompanied by rotation of the plane of polarisation of a linearly polarised probe laser, such as an argon ion laser. However, the latter has yet to be observed, and the IFE has been demonstrated only once, in the original work.[2,3] Nevertheless, it is potentially a useful new spectroscopy, because it is supported by all atoms and molecules,[7,8] and in this communication we report novel information from a computer simulation of the IFE using visible frequency laser pulses of the type available experimentally. The new information consists of a "dynamic magnetisation", measured through the angular momentum autocorrelation function (ACF) in the presence of the pump laser pulse, and second order orientational rise/fall transients.

The background theory of the IFE can be developed conveniently in terms of the magnetic dipole moment (m_i) induced by the second order product of electric field components of the electromagnetic plane wave

$$m_i = \beta_{ijk} E_j E_k \tag{1}$$

where β_{ijk} is a rank three molecular property tensor whose properties have been well described,[9–11] both classically and quantum mechanically. Specifically, it is the antisymmetric part of the tensor $E_j E_k$ that is the electromagnetic property responsible for the IFE. This is a T negative, P positive rank two tensor, conveniently

labelled π^{A}_{jk}. It follows that the P and T symmetries of β_{ijk} are both positive, so that the IFE is supported in all atoms and molecules,[12–14] thus echoing the forward Faraday effect. The analogy between the Faraday effect and the IFE is shown clearly by using the purely mathematical relation

$$\pi^{A}_{i} = \varepsilon_{ijk}\pi^{A}_{jk} \tag{2}$$

from tensor algebra. Here ε_{ijk} is the Levi Civita symbol linking the rank two antisymmetric polar tensor π^{A}_{jk} and the rank one axial tensor (i.e. axial vector) π^{A}_{i}. The latter has been shown by Wagnière[15] to be, in vector notation

$$\pi^{A} = \mathbf{E}^{+}_{L} \times \mathbf{E}^{-}_{L} = -\mathbf{E}^{+}_{R} \times \mathbf{E}^{-}_{R} = 2\mathbf{E}^{2}_{0} i\mathbf{k}\,. \tag{3}$$

Here, the subscripts denote left (L) or right (R) circular polarisation of a laser propagating in the axis Z of the laboratory frame (X, Y, Z), with $\mathbf{k}$ a unit vector in Z. The superscripts denote + and − complex conjugates of the laser plane wave.[15] It is fruitful to note that $\boldsymbol{\pi}^{A}$ in the IFE plays the role of static applied magnetic flux density ($\mathbf{B}_s$) in the forward Faraday effect, implying that there is a hitherto unobserved Zeeman splitting[16] due to a circularly polarised laser pulse, accompanied by ESR type transitions[17–20] between the pump laser induced Zeeman states. This is potentially of widespread interest in the development of optical resonance effects akin to ESR and NMR, which are also produced theoretically[21] by first order optical pumping.

The induced magnetic dipole moment m_i forms a torque with the magnetic component, $\mathbf{B}$, of the pump laser pulse

$$T_1 = -\mathbf{m} \times \mathbf{B} \tag{4}$$

whose equivalent potential energy is obtained by integration over configuration to give a contribution

$$H_1 = -\mathbf{m} \cdot \mathbf{B} \tag{5}$$

to the Hamiltonian.

We report a field applied molecular dynamics (FMD) computer simulation[22–29] of the effect of (4) or (5) in representative achiral and chiral molecular ensembles, in the rise and fall transient conditions and in the pulse-on steady state. This appears to be the first computer simulation of the IFE, the main results of which are: i) to show "dynamic magnetisation" through a non-vanishing $t \rightarrow$ infinity tail of the molecular angular momentum ACF in the axis of laser propagation; ii) to show second and higher even order orientational rise/fall transients which are given analytically for the first time and which are potentially directly observable using contemporary femtosecond modified Kerr effect apparatus.[30–33]

2. Computer Simulation

The IFE was simulated in water (C_{2v}) using a well-tested modified ST2 potential,[34–36] and in an electrically non-dipolar chiral D_2 symmetry, representing a two

bladed molecular propeller described by a Lennard Jones site model of staggered bicyclopropene (SBCP). The model consisted of six CH moieties, with Lennard Jones parameters

$$\varepsilon/k(CH) = 158\,\mathrm{K};\ \sigma(CH) = 3.8\,\text{Å}\,. \tag{6}$$

This level of approximation was considered adequate and practical for the first demonstration reported here, and can be improved for future applications with the ab initio computational potentials now becoming generally available.[37] With a time step of 0.5 fs for water and 5.0 fs for SBCP, the methods[22–29] of FMD were implemented with the torque (4) in the forces loop. For C_{2v} and D_2 point group symmetries, m_i in frame (1,2,3) of the molecular principal moments of inertia is

$$\begin{aligned} m_1 &= e_{1Z}(\beta''_{123} - \beta''_{132})E_0^2 \\ m_2 &= e_{2Z}(\beta''_{231} - \beta''_{213})E_0^2 \\ m_3 &= e_{3Z}(\beta''_{312} - \beta''_{321})E_0^2 \end{aligned} \tag{7}$$

with $\beta''_{123} = -\beta''_{132}$; $\beta''_{231} = -\beta''_{213}$; $\beta''_{312} = -\beta''_{321}$. Here e_{1Z}, e_{2Z}, e_{3Z} are Z components of unit vectors $\mathbf{e}_{1,2,3}$ in axes 1, 2, and 3. In the apparent absence of experimental and ab initio estimates of β''_{ijk}, we used for demonstration.

$$\beta''_{123} = \beta''_{231} = \beta''_{312} = 1:2:3 \tag{8}$$

for both molecules. Under these conditions, FMD simulations were completed at up to twenty visible pump laser frequencies for each 108 molecule ensemble, giving rise/fall transients and pulse-on ACF's and cross correlation functions (CCF's) at each frequency, the ACF's and CCF's being computed by running time averaging over contiguous segments of at least 6,000 time steps each for good statistics. Rise and fall transients were computed for $\langle e_{1Z}^2\rangle, \langle e_{1Y}^2\rangle, \langle e_{1X}^2\rangle, \langle e_{2Z}^2\rangle, \langle e_{2Y}^2\rangle, \langle e_{2X}^2\rangle, \langle e_{3Z}^2\rangle, \langle e_{3Y}^2\rangle, \langle e_{3X}^2\rangle$ over a range of 1,000 to 3,000 time steps by averaging over the 108 molecules at each time step. ACF's and CCF's were computed at each laser frequency for: orientation ($\mathbf{e}_1$ etc.), angular momentum ($\mathbf{J}$), and rotational velocity ($\dot{\mathbf{e}}_1$ etc.) for components X, Y, and Z.

3. Results and Discussion

FMD revealed several novel molecular dynamical aspects of the IFE. Prominent new features are illustrated in Figs. 1 and 2. Figure 1 shows the development of a $t \rightarrow$ infinity tail

$$m_\infty^2 = \frac{\langle m_Z\rangle_{t\to\infty}^2}{\langle m_Z^2\rangle} = \frac{\langle J_Z\rangle_{t\to\infty}^2}{\langle J_Z^2\rangle} \tag{9}$$

where m_Z is a pump laser induced magnetic dipole moment proportional to J_Z through a scalar. Figure 2 shows second order orientational rise/fall transients. These previously unknown features of the IFE are accompanied both in water and SBCP by orientational, angular momentum, and rotational velocity CCF's between

X and Y components, and an intricately oscillatory data bank of ACF's of each type of vector. The details of these laser induced oscillations were extremely sensitive to changes in applied laser frequency, and the data are available from the author in a bank of several hundred examples. Computer animation[38] revealed that the statistical CF patterns represent a laser driven precession of $\mathbf{J}, \dot{\mathbf{e}}_1, \dot{\mathbf{e}}_2$, and $\dot{\mathbf{e}}_3$ in competition with the thermal molecular dynamics. The level of the induced dynamic magnetisation m_∞^2 depended markedly (Table 1) on the laser frequency for both ensembles, another new feature of the IFE.

Table 1: Magnetisation m_∞^2 vs. Laser Frequency.

Normalised Magnetisation	Laser Frequency (THz)	Liquid
0.002 ± 0.02	30.0	S Bicyclopropene
0.025 ± 0.03	300.0	"
0.10 ± 0.03	450.0	"
0.55 ± 0.02	510.0	"
0.67 ± 0.03	540.0	"
0.54 ± 0.03	600.0	"
0.79 ± 0.03	630.0	"
0.76 ± 0.03	660.0	"
0.80 ± 0.02	750.0	"
0.87 ± 0.05	840.0	"
0.80 ± 0.05	900.0	"
0.88 ± 0.05	1020.0	"
0.80 ± 0.02	1200.0	"
0.65 ± 0.02	1350.0	"
0.28 ± 0.02	1500.0	"
0.00 ± 0.05	1800.0	"
0.50 ± 0.02	2400.0	"
0.90 ± 0.04	3000.0	"
0.05 ± 0.05	300.0	Water
0.02 ± 0.07	500.0	"
0.02 ± 0.06	600.0	"
0.05 ± 0.03	1000.0	"

First and higher odd order transients such as $\langle \mathrm{e}_1 \rangle$ etc. vanished for all components and laser frequencies in both ensembles. Second order rise transients such as $\langle e_Z^2 \rangle$ attained final levels which were used to construct for water a generalized Langevin/Kielich curve (Fig. 3) both analytically and from[22–29] FMD as a function of the square of the laser electric field strength in volts per metre. The analytical

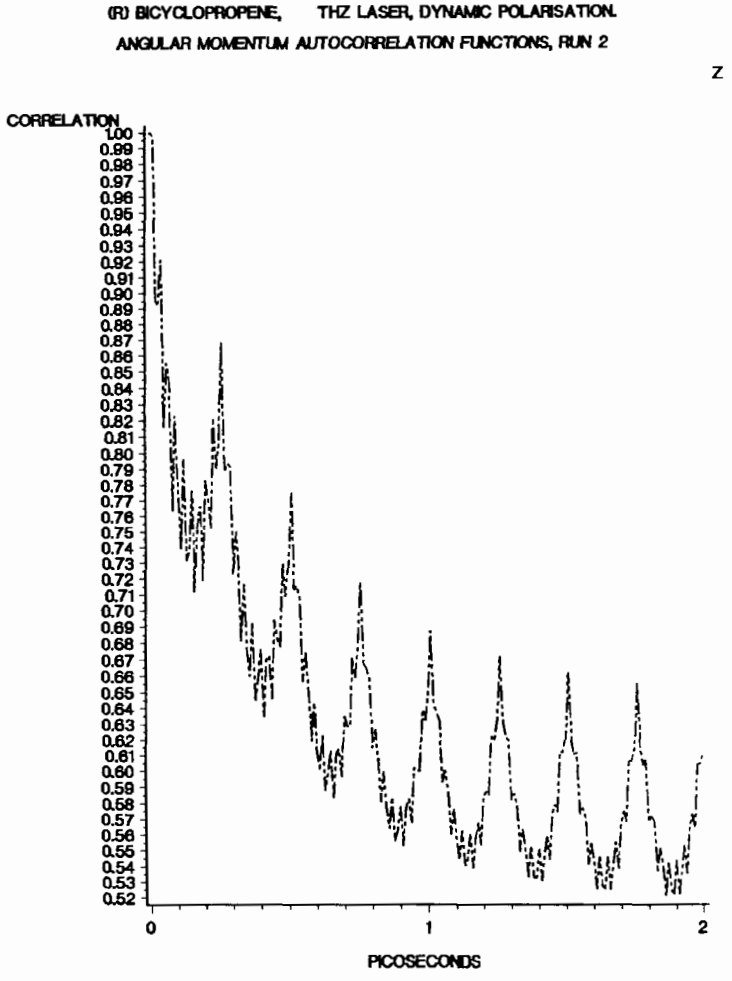

Fig. 1. Illustration in SBCP at 293 K, 1.0 bar of m_{∞}^2 dynamic magnetization in a 600 THz visible frequency laser by FMD computer simulation.

form of this function is as follows

$$\langle e_{1Z}^{n} \rangle = \frac{\int_0^{\pi} \cos^n\theta \exp(q\cos^2\theta) \int_{\exp}^{2\pi} (h\cos 2\phi(\cos^2\theta - 1))d\phi \sin\theta d\theta}{\int_0^{\pi} \exp(q\cos^2\theta) \int_0^{2\pi} \exp(h\cos 2\phi(\cos^2\theta - 1))d\phi \sin\theta d\theta} \tag{10}$$

and it is a sensitive function of the anisotropy of polarisability of water. The energy parameter q used to construct this curve (using double Gauss Legendre quadrature)

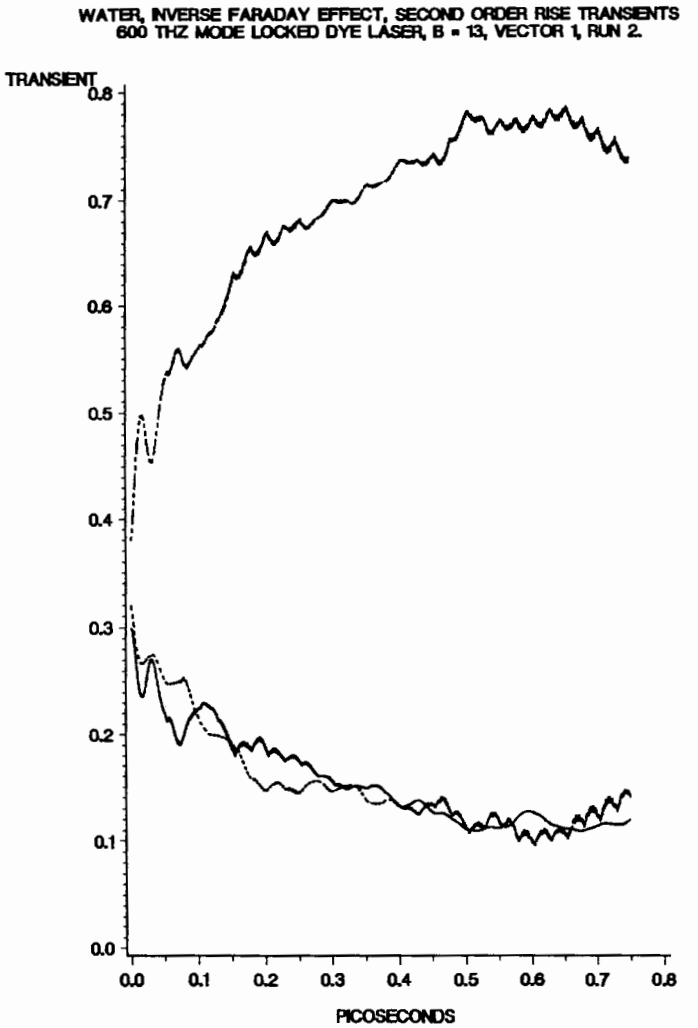

(a)

Fig. 2. Rise and fall transients $\langle e_{1Z}^2 \rangle$ in water at 293 K, 1.0 bar, by FMD at 600 THz (mode locked dye laser frequency). Laser induced internal potential energy $H_1 = 7.0\,\mathrm{kJ/mole}$. Upper curve: $\langle e_{1Z}^2 \rangle$; Lower curves: $\langle e_{1Y}^2 \rangle$ & $\langle e_{1X}^2 \rangle$.

was

$$q = \frac{E_0^2}{kT}\left(\alpha_{11} - \frac{1}{2}(\alpha_{22} + \alpha_{33})\right); \quad h = \frac{1}{2}(\alpha_{22} - \alpha_{33});$$
$$= E_0^2 \gamma / kT; \tag{11}$$

where γ is the anisotropy of polarisability of water. This curve compared well with that obtained from the computer simulation. This function represents the

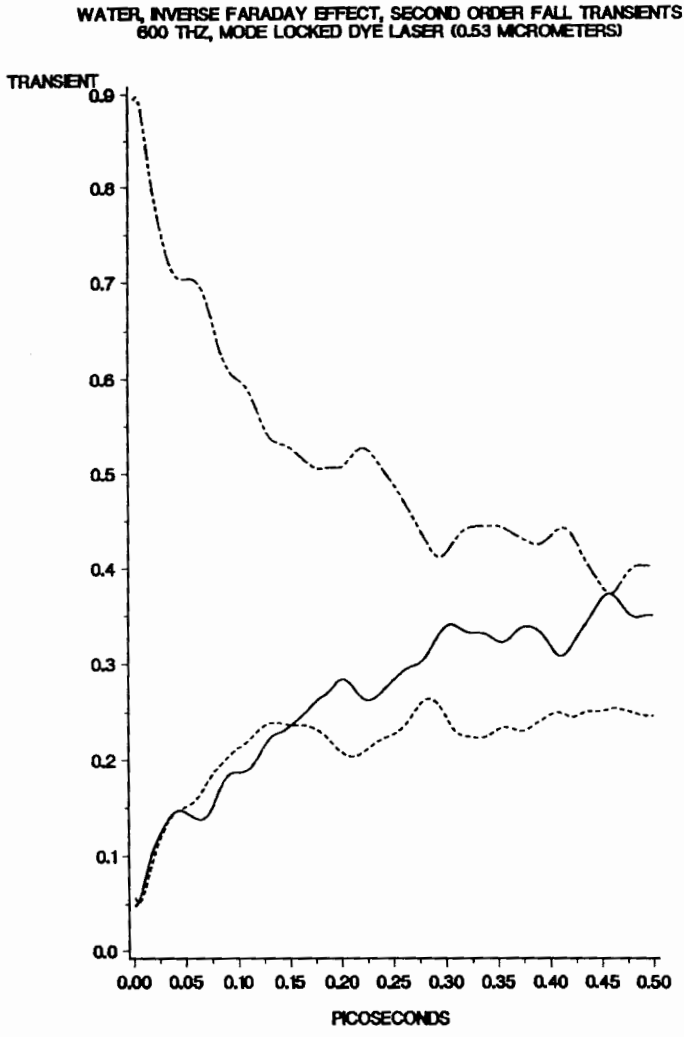

(b)

Fig. 2. (*Continued*)

development of circular birefringence in response to the laser pulse, as first proposed by Atkins and Miller.[6]

The simulated Langevin Kielich function was constructed using the computed potential energies at each laser intensity in the FMD simulation at a laser frequency of 600 THz, in the vicinity of a passively mode locked dye laser at 0.53 μm. The time dependencies of the rise/fall transients contain[22–29] much additional information on the IFE. The rise transients echoed the CF's in being sometimes intricately oscilla-

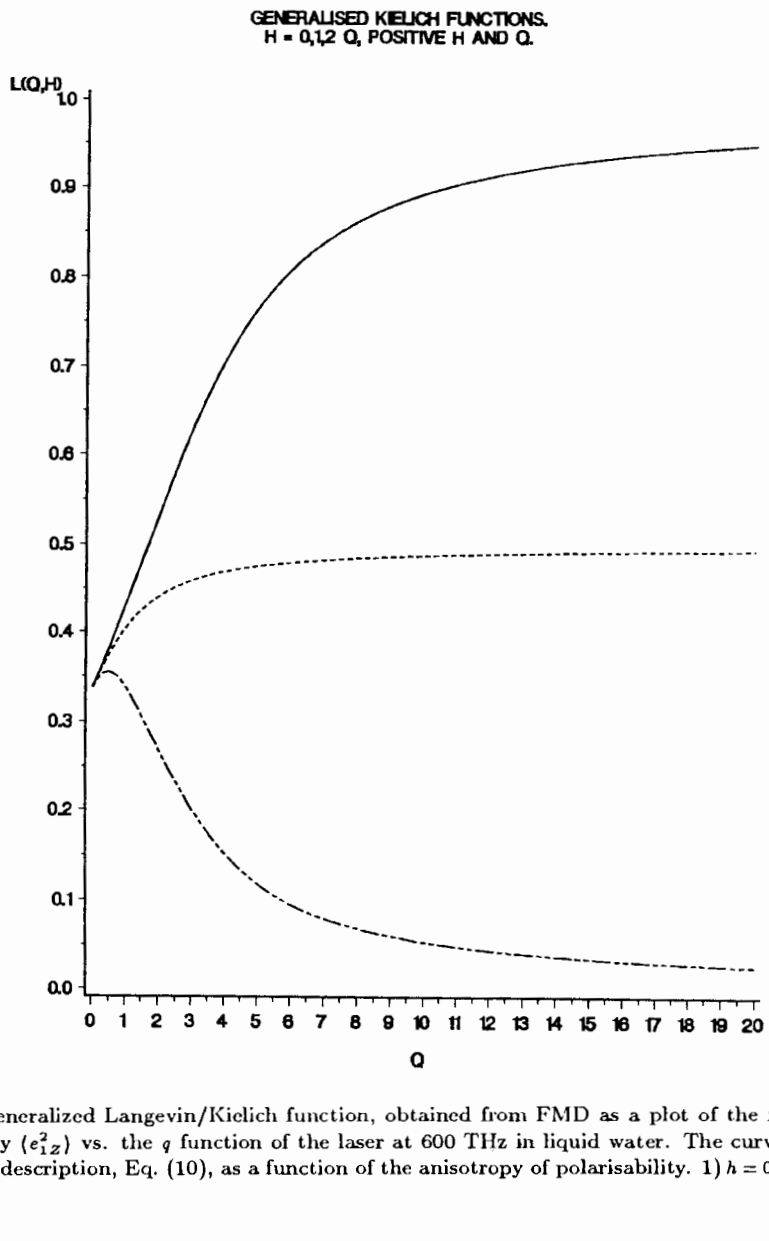

Fig. 3. Generalized Langevin/Kielich function, obtained from FMD as a plot of the final levels attained by $\langle e_{1Z}^2 \rangle$ vs. the q function of the laser at 600 THz in liquid water. The curves are our analytical description, Eq. (10), as a function of the anisotropy of polarisability. 1) $h = 0$; 2) $h = q$; 3) $h = 2q$.

tory and very sensitive to laser frequency and intensity. With the time resolution of contemporary femtosecond spectroscopy[30–33] these patterns are probably directly observable. One method would be to modify optical Kerr effect apparatus[33] to observe the additional transient effect of circularly polarising the pump laser pulse as the rotation of the plane of linear polarisation of an argon ion probe. To observe the IFE transient, subtract the transient due to the optical Kerr effect, which occurs

when the pump laser is unpolarised. The IFE occurs only when the pump laser is circularly polarised.

4. Summary

Several novel features of the IFE have been observed by FMD, including dynamic magnetisation (Table 1) and even order rise/fall transients signalling the onset of circular birefringence. The latter have been analysed with the use of the Langevin/ Kielich functions of statistical mechanics.

Acknowledgments

Prof. Dr. G. Wagnière and the Swiss NSF is thanked for an invitation to the University of Zurich. Animations were carried out at Cornell Theory Center, which receives major funding from NSF (US), IBM (US), IBM (US), New York State, and members of the Corporate Research Institute. Dr. Laura J. Evans is thanked for invaluable help with the SAS plotting facilities of the Irchel mainframe, used to build up the data bank. ETH Zurich is thanked by MWE for the award of a major computing grant on the IBM 3090 computer, with which the FMD simulations were carried out. Prof. S. Wozniak is thanked for many interesting discussions on the Langevin Kielich function.

References

1. P. S. Pershan, *Phys. Rev.* **130**, 919 (1963).
2. J. P. van der Ziel, P. S. Pershan, and L. D. Malmstrom, *Phys. Rev. Lett.* **15**, 190 (1965).
3. J. P. van der Ziel, P. S. Pershan, and L. D. Malmstrom, *Phys. Rev.* **143**, 574 (1966).
4. M. W. Evans, *Phys. Rev. Lett.* **64**, 2909 (1990).
5. M. W. Evans, *Opt. Lett.* **15**, 863 (1990).
6. P. W. Atkins and M. H. Miller, *Mol. Phys.* **15**, 503 (1968).
7. P. W. Atkins, *Molecular Quantum Mechanics*, second edition (Oxford Univ. Press, 1983).
8. Y. R. Shen, *The Principles of Non-Linear Optics* (Wiley, 1984).
9. L. D. Barron, *Molecular Light Scattering and Optical Activity* (Cambridge Univ. Press, 1982).
10. S. Kielich, in *Dielectric and Related Molecular Processes*, (Chem. Soc., London, 1972), Vol. 1.
11. S. Wozniak, *Mol. Phys.* **59**, 421 (1986).
12. S. Kielich, "Nonlinear Molecular Optics" (Nauka, 1981).
13. L. D. Barron and J. Vrbancich, *Mol. Phys.* **51**, 715 (1984).
14. S. Wozniak, B. Linder, and R. Zawodny, *J. Phys. (Paris)* **44**, 403 (1983).
15. G. Wagnière, *Phys. Rev.* **A40**, 2437 (1989).
16. M. W. Evans, *J. Mol. Spectr.* **143**, 327 (1990).
17. M. W. Evans, *J. Mol. Opt.* **37**, 1655 (1990).
18. M. W. Evans, *J. Phys. Chem.* in press.
19. W. S. Warren, Department of Chemistry, Princeton Univ., personal communications concerning the prototype experiment.
20. M. W. Evans, *Spectrochim. Acta* **46A**, 1475 (1990).

21. Ref. 8, chapter 5.
22. M. W. Evans, *J. Chem. Phys.* **76**, 5473, 5480 (1982).
23. M. W. Evans, *J. Chem. Phys.* **77**, 4632 (1982); *ibid.* **78**, 925, 5403 (1983).
24. M. W. Evans, W. T. Coffey, and P. Grigolini, *Molecular Diffusion*, (Wiley Interscience, 1984; 2nd edition, MIR, 1988).
25. M. W. Evans, in *Advances in Chemical Physics*, ed. M. W. Evans, P. Grigolini, G. Pastori, I. Prigogine, and S. A. Rice (Wiley Interscience, 1985), Vol. 62.
26. M. W. Evans, G. C. Lie, and E. Clementi, *Chem. Phys. Lett.* **138**, 149 (1987).
27. M. W. Evans, G C. Lie, and E. Clementi, *Phys. Rev.* **A36**, 226 (1987); *ibid.* **37**, 2548, 2551 (1988).
28. M. W. Evans and G. Wagnière, *Phys. Rev.* **A42**, 6732 (1990).
29. M. W. Evans, in *Advances in Chemical Physics*, ed. I. Prigogine and S. A. Rice (Wiley Interscience, 1991), Vol. 81, in press, review with 450 references.
30. D. C. Hanna, M. A. Yuratich, and D. Cotter, *Non-Linear Optics of Free Atoms and Molecules* (Springer, 1979).
31. G. Kenney Wallace in *Advances in Chemical Physics*, ed. I. Prigogine and S. A. Rice (Wiley Interscience, 1982), Vol. 47.
32. S. Feneuille, *Rep. Prog. Phys.* **40**, 1257 (1977).
33. H. J. Coles and B. R. Jennings, *Mol. Phys.* **31**, 571 (1976).
34. M. W. Evans, *J. Mol. Liq.* **32**, 173 (1986).
35. M. W. Evans, G. C. Lie, and E. Clementi, *J. Chem. Phys.* **88**, 5157 (1988).
36. M. W. Evans, G. C. Lie, and E. Clementi, *J. Chem. Phys.* **87**, 6040 (1987).
37. E. Clementi MOTECC 1989/1990 (Escom, Leiden, 1989, 1990).
38. C. R. Pelkie, animation consultant, Cornell Theory Center.